Fluid Phase Equilibria 510 (2020) 112495

Contents lists available at ScienceDirect

Fluid Phase Equilibria

journal homepage: www.elsevier.com/locate/fluid

Liquid-liquid phase transition in simple Lennard-Jones nano-confined fluids

Narjes Sheibani , Mohammad Kamalvand *

Department of Chemistry, Faculty of Science, Yazd University, Yazd, 89195-741, Iran

A R T I C L E I N F O

Article history:
Received 8 August 2019
Received in revised form
18 January 2020
Accepted 20 January 2020
Available online 22 January 2020

Keywords:
Confined fluid
Liquid-liquid phase transition
Nano-slit

A B S T R A C T

In this study, the phase transition of confined argon in slit by Lennard-Jones (12-6) potential for fluids-fluids and walls-fluids interactions is investigated. The effects of temperature, pressure, and distance between the two walls on the phase transition were investigated by using the molecular dynamics simulation and LAMMPS software. It was found that wall distances had a significant effect on phase transition. Although the molecules were spherical and the walls structureless, liquid-liquid phase transition was observed when wall distances were approximately 3σ; that is, confinement had a determining role in phase transition in confined fluids.

1. Introduction

Recently, the behavior of confined fluids in the nanometer-size group of systems has been of interest to researchers because of abundant applications in the fields of nanoscience and nanotechnology. Therefore, it is important to know the properties of the confined fluids in nano-systems, which are significantly different from macroscopic fluids [1].

Thermodynamic properties of the confined fluids, because of the limitations of nanopores as well as interactions between the walls and particles are very different from those of macroscopic fluids. The effects of temperature and pressure on the confined fluids of argon and krypton in nanopores with poor adsorption and those with hard walls have been investigated [2]. Also, a similar study was conducted with amorphous silica walls using the Monte Carlo simulation [3].

So far, many studies have been carried out on fluids by molecular dynamics simulation [4–9] and theoretical methods [10–19] aimed at understanding how to change the phase diagram by confinement as well as at evaluating the confined fluid structure. The phase behaviors of vapor-solid, liquid-vapor, and liquid-solid with argon in graphite nanopores of sizes 1–8 nm were studied by using Monte Carlo simulation and meso-canonical ensemble [20].

A solid-solid phase transition occurs only in the solid phase and differs from crystallization and melting processes. By changing temperature or pressure, a crystalline solid can be transformed into another form of crystalline solid without entering the liquid phase, which results in the pleomorphic form of the material [21]. Changes in the triangular structure and square structure, as well as the solid-solid phase transition, were addressed by confining the Lennard-Jones soft sphere in nanopores using Monte Carlo simulation [20]. Then, by applying the DFT theory, solid-solid phase transition was investigated in triangular and square crystalline structures for thin layers with graphite surfaces and the obtained data were compared with the results of simulation [22,23]. Furthermore, by using Monte Carlo simulations in nanopores with wall distances of 2–6 times of molecular diameter, surveying the solid-liquid and solid-solid phase transitions, and considering various types of structures such as fcc and hcp, crystals and solids in this system were investigated and the results were made consistent by the Clapeyron equation for the nanopores [24].

Recently, experimental and simulation results showed crystal-like arrangements in the liquid phase. The theory of liquid states declares that the arrangement of atoms in the liquid is likely to be in the following two forms [25]:

- The major portion of the atoms appertain to a multiply linked district of the “perfect matter; ”
- The remainder of the atoms appertains to spot-like and linear defects, which are the complement of the “perfect matter” district with respect to the complete space.

* Corresponding author.
E-mail address: kamalvand@yazd.ac.ir (M. Kamalvand).

https://doi.org/10.1016/j.fluid.2020.112495
0378-3812/

The structure of the main region is almost crystalline and a change in the arrangement of atoms can lead to the formation of a liquid with different densities, which is referred to as liquid-liquid transition [25]. The liquid-liquid phase transition between two Lennard-Jones fluids, which can almost be dissolved, has been studied [26]. In addition to studies on liquid-liquid phase transition for water [27], some investigations have carried out into the liquid-liquid phase transition for water confined in nanopores of silica [28]. However, so far, liquid-liquid phase transitions have not been investigated for confined argon in the slit. Thus, this study has been conducted for confined argon in slit with amorphous walls to show that even in simple systems, the liquid-liquid phase transition is observable. This means that it does not occur only in complex systems.

In this work, we investigated the pressure and temperature effects on the confined fluid phase transition. In order to study liquid-liquid phase transition, the effect of distance between two walls was investigated on argon confined in a slit in the liquid phase.

2. Simulation method

There are not many theories to investigate the behavior of confined fluid because of their complexity [24], so using simulation to study these systems is usual. Today, due to advances in the computer technology, and while simulation methods are safe, controllable and low cost, relative to the experimental methods, are of great advantage. Usually, the results of the simulation are in agreement with the experimental results, which makes it a good way to test the systems. LAMMPS is one of the oldest and most successful molecular dynamics codes that has the capability to simulate high-particle systems. Therefore, in this study we used LAMMPS to investigate the phase transition in confined argon.

To study the phase transition, we simulated a box with x,y = 180σ, which were periodic, and z varied from 2σ to 5σ, which was nonperiodic (fixed), where σ is the fluid molecules diameter. σ and ε/k_B in this simulation were 3.405 Å and 117.7 K (the same as argon), respectively, and the cutoff was set to 5σ. Considering the effect of the number of atoms on the results of simulation, 40000 argon atoms, which we found to be suitable for obtaining acceptable results, were considered. NPT MD simulation was run in LAMMPS [29]. Pressure in x and y directions and temperature were controlled by Berendsen barostat and Nose-Hover thermostat, respectively and reduced relaxation times were 0.5 and 5 for temperature and pressure, respectively. The number of timesteps was 2000000 to reach equilibrium and 1500000 to perform the sampling and reduced timestep was 0.004. Because our focus was on the effects of temperature, pressure, and wall distance on the Lennard-Jones fluid, wall-fluid interactions were considered as fluid-fluid interactions with LJ 12-6 with cutoff of 3σ. This should be noted that the whole interface distance in the z-direction, H, is not accessible for fluid molecules. Therefore, the accessible distance between two walls is approximately H-σ.

3. Results and discussion

In order to investigate the effect of pressure on confined fluid phase transition, the density-temperature diagram was drawn in three distances of walls, namely $H = 2.8\sigma$, 3σ, and 3.2 with reduced pressures (in x and y direction) of 0.0016 (0.68 atm, which is the pressure of the triple point of the bulk), 0.024 (10 atm), 0.049 (20 atm), and 1.00 (400 atm) and reduced temperature range of 0.2–1.4 (24–165 K), as shown in three dimensions in Fig. 1. From Fig. 1, it can be deduced that a small change in the distance of walls leads to a tangible change in the phase transition, which is clear in the solid-liquid and liquid-gas phase transitions for slits with $H =$ 2.8σ-3.2σ. We can clearly observe the solid-liquid and liquid-gas phase transitions with $H = 3.2\sigma$ and $H = 2.8\sigma$. Also, with $H = 3\sigma$, the solid-liquid phase transition is detectable, but there is no clear evidence for liquid-gas phase transition. In addition, for reduced pressure of 0.0016 (0.68 atm) and reduced temperature of 0.5–0.7 (60–80 K), the slope is sharp and the discontinuity represents sublimation. When pressure increases, solid density also increases and the slope is reduced in temperatures between 0.5 and 0.7 (60–80 K). In high pressures, e.g., reduced pressure of 1 (400 atm), there is only one discontinuity; from this, it can be concluded that in this temperature range, only solid-liquid phase transition is

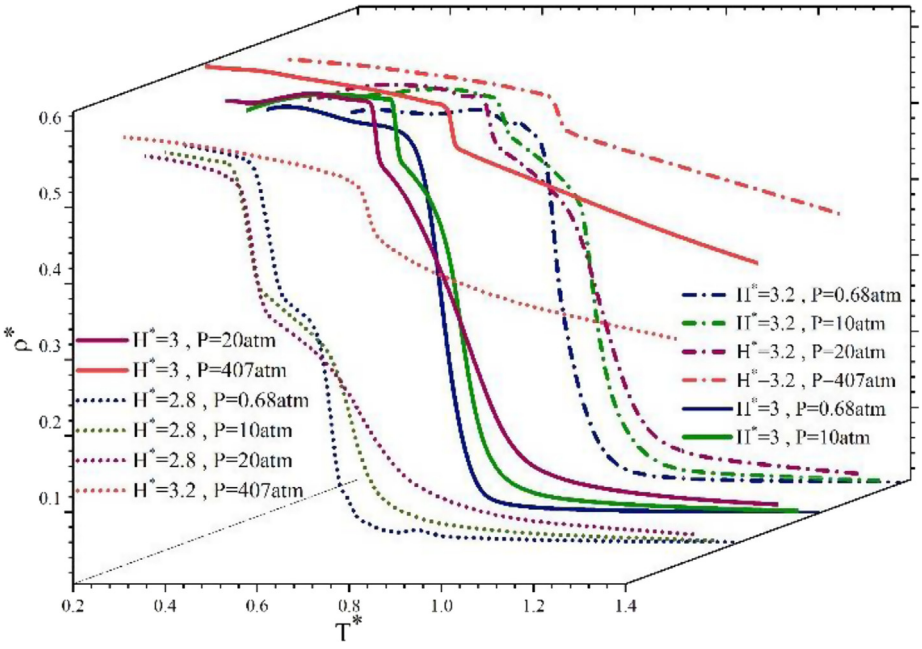

Fig. 1. Reduced density as a function of reduced temperature with $H = 2.8$, 3, and 3.2σ and $P^* = 0.0016$ (0.68 atm), 0.024 (10 atm), 0.049 (20 atm), and 1 (400 atm).

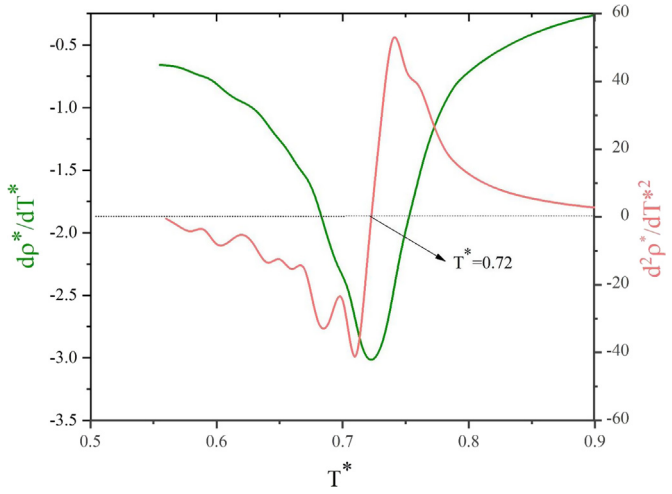

Fig. 2. First and second derivatives of reduced density as a function reduced the temperature with P* = 0.049 (20atm) and H = 3σ.

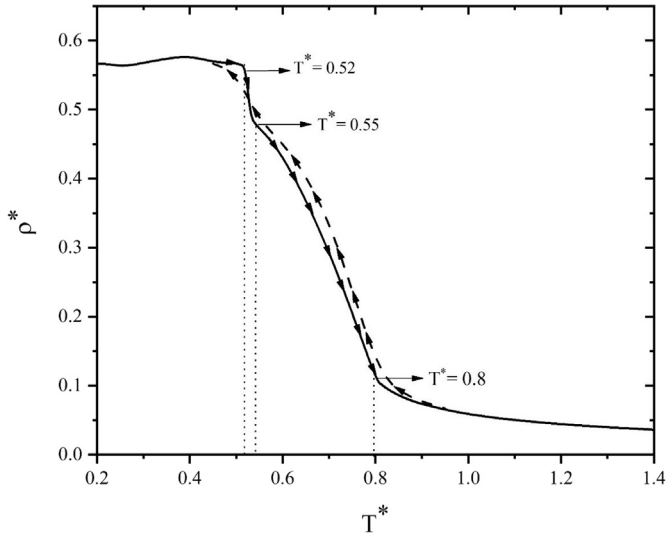

Fig. 3. Reduced density as a function of reduced temperature and its hysteresis for P* = 0.049 (20 atm) and $H = 3\sigma$.

observed and liquid-gas phase transition may occur at higher temperatures.

In reduced pressure of 0.0016 (0.68 atm), there is one discontinuity, which indicates that this pressure and temperature are lower than those in the triple point of bulk argon and we have a first-order phase transition. It was observed that for reduced pressure of 0.049 (20 atm) and reduced temperature between 0.55 and 0.9 (65 and 106 K), the second numerical derivative of the density-temperature curve had discontinuity at T* = 0.72 (85 K), representing liquid-gas phase transition, as shown in Fig. 2. It should be noted that the first-order liquid-gas phase transition is seen at 130 K for a non-confined argon at pressure 20 atm. Also, for a reduced pressure of 0.024 (10 atm), the second numerical derivative discontinuity was seen at T* = 0.65 (77 K); this showed that the effect of pressure was more on the liquid-gas phase transition than on solid-liquid phase transition, like in macroscopic fluids. It should be noted that in first-order phase transition, the first derivatives of chemical potential have discontinuity and in second-order phase transition, the second derivatives of chemical potential have discontinuity [30].

In order to investigate the effect of temperature, we drew density-temperature, enthalpy-temperature, and P_{zz}-temperature diagrams, which are shown in Figs. 3–5, respectively. In addition, hysteresis was plotted on the density-temperature diagram. Discontinuities represent the first-order phase transitions in reduced temperature range of 0.52–0.55 (63–65 K).

In Figs. 3–5, it can be seen that in the reduced temperatures of 0.52, 0.55, and 0.8 (63, 65, and 94 K), significant changes in the trend occur. For the three temperatures, RDFs are plotted in Fig. 6. At T* = 0.52 (63 K), RDF is similar to solid RDF and at T* = 0.55 (65 K), it is similar to liquid RDF, indicating the occurrence of solid-liquid phase transition. At T* = 0.80 (94 K), RDF is similar to gas RDF, because can be seen as one weak layer in RDF.

Local density profile is presented in Fig. 7 for these temperatures. At the reduced temperature of 0.52 (63 K), atom densities are higher near the walls and there is no atom in the middle part of the box; thus, the system is solid. At the reduced temperature of 0.55 (65 K), atom densities decrease near the walls and it is possible to

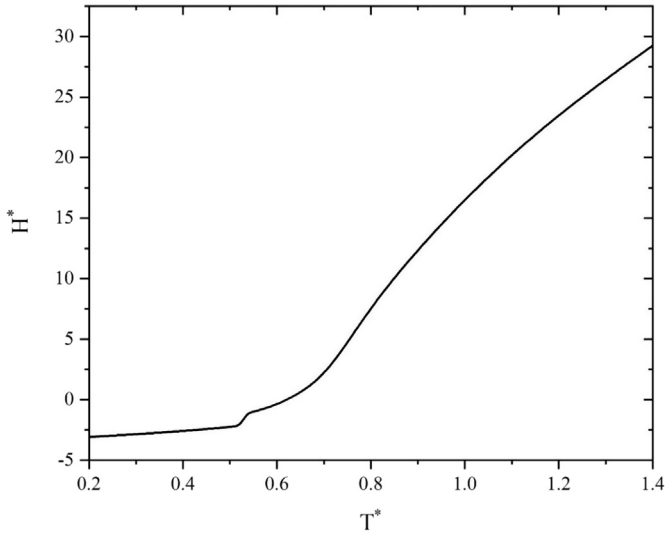

Fig. 4. Reduced enthalpy as a function of reduced temperature for P* = 0.049 (20 atm) and $H = 3\sigma$.

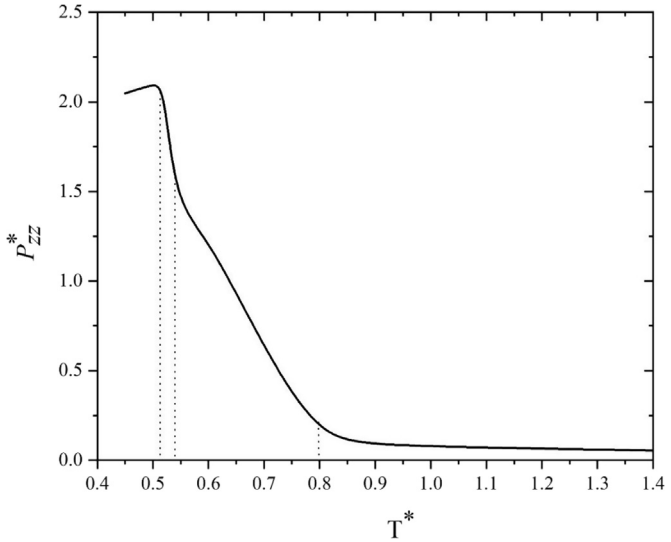

Fig. 5. Reduced normal pressure as a function of reduced temperature for P* = 0.049 (20 atm) and $H = 3\sigma$.

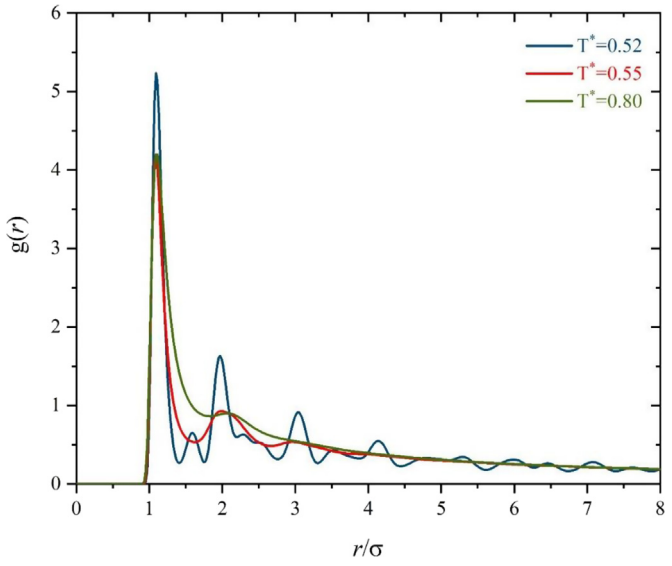

Fig. 6. Pair correlation function g(r) for three reduced temperatures in three phases; T* = 0.52(63K) for solid, T* = 0.55 (65K) for liquid, and T* = 0.80 (94K) for gas with P* = 0.049 (20 atm) and $H = 3\sigma$.

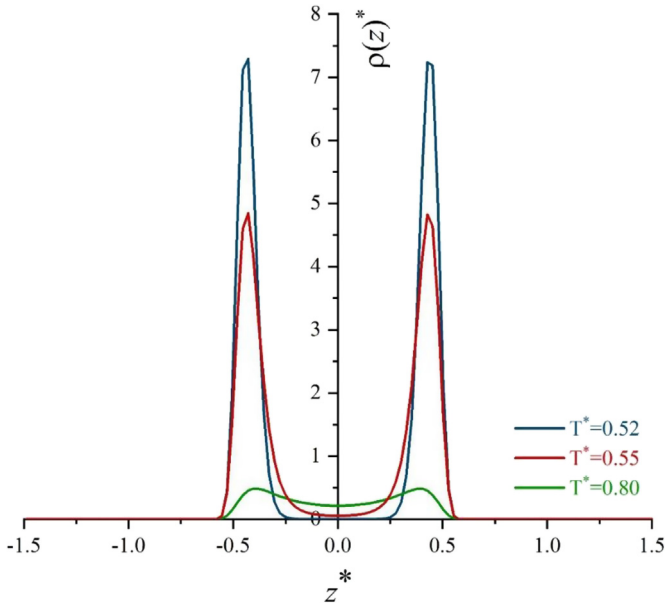

Fig. 7. Local density profile for three reduced temperatures in three phases; T* = 0.52 (63 K) for solid, T* = 0.55 (65 K) for liquid, and T* = 0.80 (94 K) for gas with P* = 0.049 (20 atm) and $H = 3\sigma$.

observe particles in the central part between the two walls; therefore, the system may be liquid. At the reduced temperature of 0.8 (94 K), particles are present in almost all of the parts between the two walls and they do not have any specific order; this behavior is similar to the behavior of gaseous argon.

We also checked the order parameter to proof the solid-liquid phase transition. The order parameter can be obtained in the following manner from the MD form-data:

$$\Psi_k = \frac{1}{N_b}\left|\sum_{j=1}^{N_b}\exp(ik\theta_j)\right| \quad (1)$$

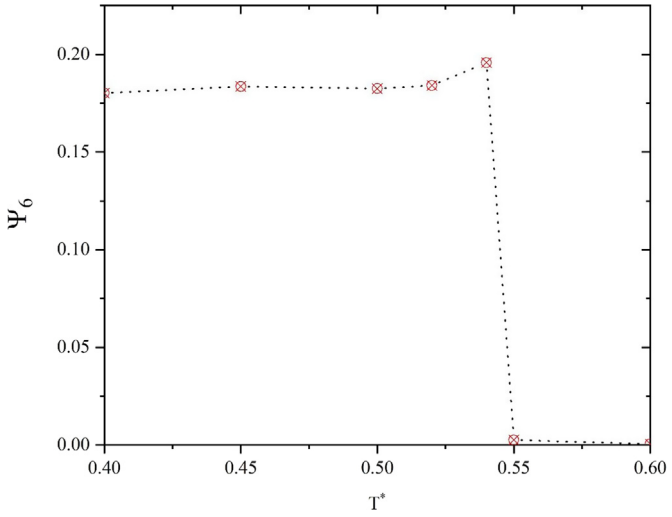

Fig. 8. Order parameter as a function of reduced temperature for P* = 0.049 (20 atm) and $H = 3\sigma$.

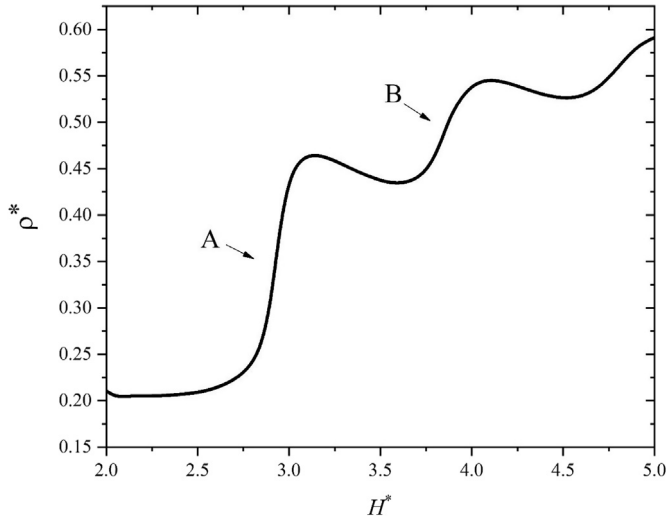

Fig. 9. Reduced density as a function distance between walls for T* = 0.6 (70K), i.e., in the liquid state, at P* = 0.049 (20atm).

That N_b is the total number of near neighbors, θ_j is the angle formed by a particle with its nearest neighbor atom. The value of Ψ_k differs between 0 and 1 also k can be between 2 and 6 that in this paper considered $k = 6$ because the value of others was negligible. A distance cutoff of 3σ was used while computing the nearest neighbors. The results for the order parameter are shown in Fig. 8. As can be seen at T* = 0.52, the reported temperature for solid-state, the order parameter has a significant value due to the order in the solid structure and at T* = 0.55, the reported temperature for liquid, this parameter is approximately zero that confirms the solid-liquid phase transition between T* = 0.52–0.55 that is in good agreement with other results reported in Figs. 3–7.

We choose T* = 0.6 (70 K), which is suitable to study the liquid-liquid phase transition at 20 atm because of the density-temperature diagram in Fig. 3 was in liquid range. The density-walls distances diagram in the range of 2-5σ, is shown in Fig. 9. There are two discontinuities in this diagram. For region A in the range of 2.85σ 2.95σ, RDF and local density are investigated and shown in Fig. 10. RDFs are similar to liquid RDF for both slits.

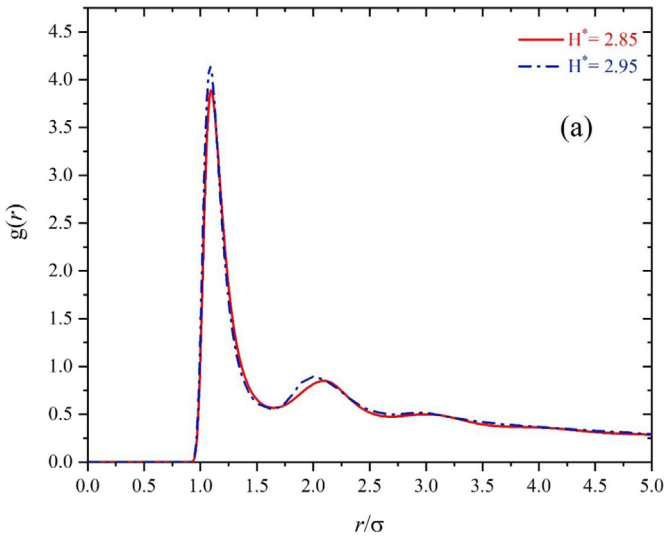

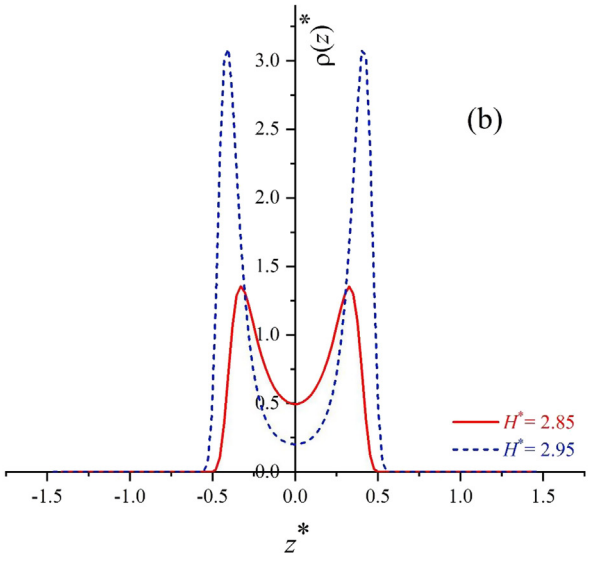

Fig. 10. (a) Pair correlation function g(r) and (b) local density for region A in Fig. 9.

However, local density profile and atom arrangement change; therefore, we observe two liquids with different densities in both distances. In addition, density is not zero in the middle part between two peaks and there are atoms in this distance; thus, argon is liquid. From the mentioned evidence, it can be concluded that the first-order liquid-liquid phase transition occurs in region A when $H \approx 2.9\sigma$.

In Fig. 11, the first numerical derivative of density versus wall distance is plotted for region B in Fig. 9. A discontinuity is observed between wall distances of 3.84σ and 3.86σ, as shown in Fig. 11. Also, RDF and local density are investigated for both distances in Fig. 12. From Fig. 12a it is observed that RDF diagrams are similar to liquid RDF. But, from Fig. 12b local density and atom arrangement change and two liquids with different densities are present in the two distances. In addition, the diagram shows three peaks, which are due to the presence of particles in the middle part; thus, argon is liquid. The order parameter was calculated for these distances and was approximately zero, which can certify that both systems are liquid. From the evidence, it can be concluded that the second-order liquid-liquid phase transition occurs in region B of Fig. 9.

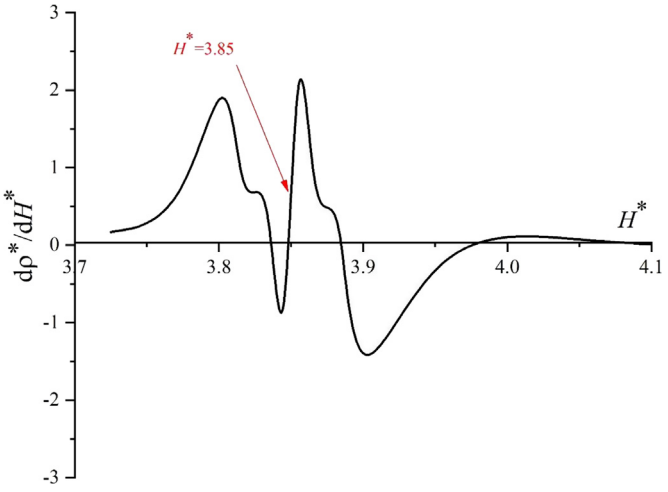

Fig. 11. The first derivative of density-wall distance for part B in Fig. 9.

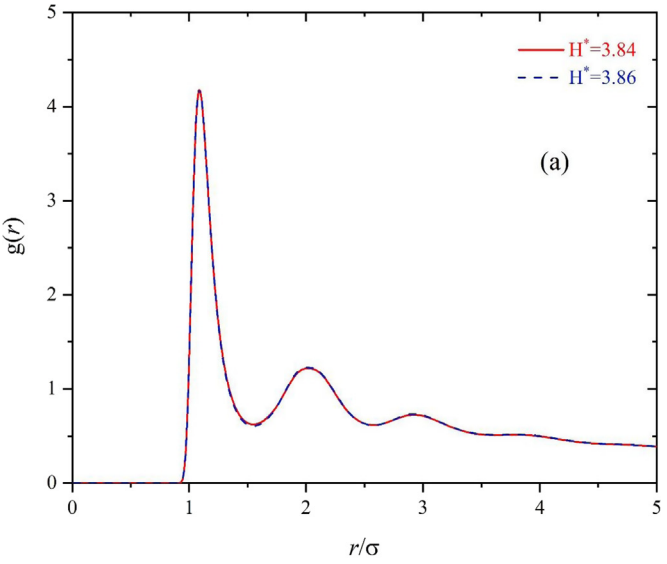

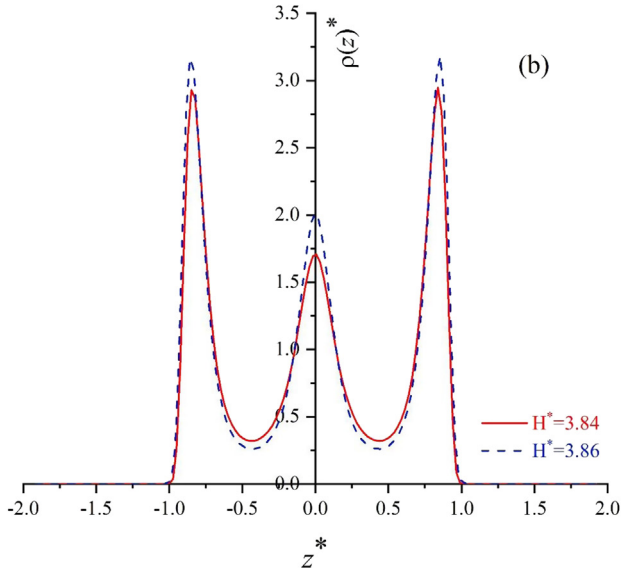

Fig. 12. (a) Pair correlation function g(r) and (b) local density for part B in Fig. 9.

4. Conclusion

In this study, we investigated the effects of temperature, pressure, and distance between two walls on phase transition of confined argon in slit. An increase in temperature led to a change of density, causing a phase transition of confined argon in the slit. In the investigation into the effect of pressure and slit size, H, results showed that a small change in the distance between walls would lead to a tangible change in the phase transition at reduced pressures of 0.0016 (0.68 atm), 0.024 (10 atm), 0.049 (20 atm), and 1 (400 atm) with three wall distances of 2.8, 3, and 3.2σ and in the reduced temperature range of 0.2−1.4 (24−165 K). The solid-liquid and liquid-gas phase transitions were clear at $H = 2.8\sigma$. We clearly observed solid-liquid and liquid-gas phase transitions at $H = 3.2\sigma$ and $H = 2.8\sigma$. Also, at $H = 3\sigma$, the solid-liquid phase transition was detectable and it was observed at $T^* = 0.52$ (61 K); however, there were no clear evidences of liquid-gas phase transition and high-order phase transition was observable at $T^* = 0.72$ (85 K). In the investigation into the effect of distance between two walls, we chose $T^* = 0.6$ (70 K) to study the liquid-liquid phase transition at 20 atm. Because the density-temperature diagram was in the liquid range, we plotted density-wall distance for wall distance range of 2-5σ and observed two liquid-liquid phase transitions. One of them was first-order and within $H^* = 2.85$−2.95 and the other was second-order and at $H^* = 3.85$. Therefore, we can concluded that the liquid-liquid phase transition, in addition to fluids with complex molecules, can be happened in simple fluids with spherical molecules, due to confinement.

Declaration of competing interest

The authors declare that they have no known competing financial interests or personal relationships that could have appeared to influence the work reported in this paper.

CRediT authorship contribution statement

Narjes Sheibani: Writing - original draft, Data curation. **Mohammad Kamalvand:** Writing - original draft, Data curation, Supervision.

Acknowledgment

The authors wish to thank the support from Yazd University, Iran.

List of symbols

DFT	Density functional theory
NPT	Ensamble with constant Number of particles, Pressure and Temperature
fcc	Face centered cubic
hcp	hexagonal closest packed
RDF	Radial distribution function
MD	Molecular dynamic
x,y,z	Box dimensions
σ	Molecule diameter
ε	Depth of potential wells
k_B	Boltzmann constant
H^*	Reduced distance between two walls
T^*	Reduced temperature
ρ^*	Reduced density
P^*	Reduced pressure
Ψ_k	Order parameter
N_b	total number of near neighbors
θ_j	the angle formed by a particle with its nearest neighbor atom
$g(r)$	Pair correlation function

References

[1] T. Keshavarzi, R. Sohrabi, G.A. Mansoori, An analytic model for nanoconfined fluids phase-transition: applications for confined fluids in nanotube and nanoslit, J. Comput. Theor. Nanosci. 3 (2006) 134−141.
[2] A. Sengupta, J. Adhikari, A grand canonical Monte Carlo simulation study of argon and krypton confined inside weakly attractive slit pores, Mol. Simulat. 41 (2015) 402−413.
[3] X. Yang, X. Yue, Adsorption and structure of Lennard−Jones model fluid in slit-like amorphous silica nanopores, Colloids Surf., A 301 (2007) 166−173.
[4] B.K. Peterson, K.E. Gubbins, Phase transitions in a cylindrical pore: grand canonical Monte Carlo, mean-field theory and the Kelvin equation, Mol. Phys. 62 (1987) 215−226.
[5] J.P.R.B. Walton, N. Quirke, Capillary condensation: a molecular simulation study, Mol. Simulat. 2 (1989) 361−391.
[6] S.G. Heffelfinger, Z. Tan, K.E. Gubbins, U.M.B. Marconi, F. Van Swol, Lennard-Jones Mixtures in a Cylindrical Pore. A comparison of simulation and density functional theory, Mol. Simulat. 2 (1989) 393−411.
[7] V. Vadhana, K.G. Ayappa, Structure and dynamics of octa methyl cyclo tetra siloxane confined between mica surfaces, J. Phys. Chem. B 120 (2016) 2951−2967.
[8] C.Z. Qiao, S.L. Zhao, H.L. Liu, W. Dong, Connect the thermodynamics of bulk and confined fluids: confinement-adsorption Scaling, Langmuir 35 (2019) 3840−3847.
[9] M. Rajasekaran, K.G. Ayappa, Enhancing the dynamics of water confined between graphene oxide surfaces with janus interfaces: a molecular dynamics study, J. Phys. Chem. B 123 (2019) 2978−2993.
[10] R. Evans, U.M.B. Marconi, P. Tarazona, Capillary condensation and adsorption in cylindrical and slit-like pores, J. Chem. Soc. Faraday. Trans. 2 (82) (1986) 1763−1787.
[11] M.E. Fischer, H. Nakanishi, Scaling theory for the criticality of fluids between plates, J. Chem. Phys. 75 (1981) 5857−5863.
[12] U.M.B. Marconi, F. Van Swol, Microscopic model for hysteresis and phase equilibria of fluids confined between parallel plates, Phys. Rev. A 39 (1989) 4109.
[13] A. Trokhymchuk, D. Henderson, A. Nikolov, D.T. Wasan, A simple calculation of structural and depletion forces for fluids/suspensions confined in a film, Langmuir 17 (2001) 4940−4947.
[14] E. Keshavarzi, M. Kamalvand, Energy effects on the structure and thermodynamic properties of nanoconfined fluids (A density functional theory study), J. Phys. Chem. B 113 (2009) 5493−5499.
[15] G.A. Mansoori, S.A. Rice, Confined fluids: structure, properties and phase behavior, Adv. Chem. Phys. 156 (2014) (chapter 5).
[16] D. Srivastava, E.E. Santiso, K.E. Gubbins, Pressure enhancement in confined fluids: effect of molecular shape and fluid-wall interactions, Langmuir 33 (2017) 11231−11245.
[17] A. Helmi, Z. Vosoughi, Effects of quantum correction on the density profile, adsorption, and phase behavior of confined hydrogen and deuterium fluids in small systems: a DFT study, Fluid phase. Equilib 491 (2019) 24−34.
[18] K. Zhang, N. Jia, L. Liu, Adsorption thicknesses of confined pure and mixing fluids in nanopores, Langmuir 34 (2018) 12815−12826.
[19] G.A. Mansoori, E. Keshavarzi, Recent developments in phase transitions in small/NanoSystems, Adv. Phytonanotechnol. (2019) 1−16.
[20] P. Phadungbut, D.D. Do, D. Nicholson, C. Tangsathitkulchai, On the phase transition of argon adsorption in an open-end slit pore-effects of temperature and pore size, Chem. Eng. Sci. 126 (2015) 257−266.
[21] S.Z. Cheng, Phase Transitions in Polymers: the Role of Metastable States, Elsevier, 2008.
[22] K. Ayappa, C. Ghatak, The structure of frozen phases in slit nanopores: a grand canonical Monte Carlo study, J. Chem. Phys. 117 (2002) 5373−5383.
[23] H. Bock, K. Gubbins, K. Ayappa, Solid/solid phase transitions in confined thin films: a zero temperature approach, J. Chem. Phys. 122 (2005), 094709.
[24] T. Kaneko, T. Mima, K. Yasuoka, The Phase diagram of Lennard-Jones fluid confined in slit pores, Chem. Phys. Lett. 490 (2010) 165−171.
[25] A. Mitus, A. Patashinskii, B. Shumilo, The liquid-liquid phase transition, Phys. Lett. 113 (1985) 41−44.
[26] J.B. Buhn, P.A. Bopp, M.J. Hampe, A molecular dynamics study of a liquid-liquid interface: structure and dynamics, Fluid Phase Equil. 224 (2004) 221−230.
[27] S. Buldyrev, G. Franzese, N. Giovambattista, G. Malescio, M. Sadr-Lahijany, A. Scala, A. Skibinsky, H. Stanley, Models for a liquid-liquid phase transition, Physica A 304 (2002) 23−42.
[28] Z. Wang, K. Ito, J.B. Leão, L. Harriger, Y. Liu, S.H. Chen, Liquid-liquid phase transition and its phase diagram in deeply-cooled heavy water confined in a nanoporous silica matrix, J. Phys. Chem. Lett. 6 (2015) 2009−2014.
[29] C.K. Das, J.K. Singh, Melting transition of confined Lennard-Jones solids in slit pores, Theor. Chem. Acc 132 (2013) 1351−1364.
[30] P.W. Atkins, J. De Paula, Physical Chemistry, Oxford University Press, 2006 (chapter 4), section 6.